PREDICTED AND MEASURED RESPONSE OF FLEXIBLE CYLINDERS IN SHEARED FLOW

by

J. Kim Vandiver
Massachusetts Institute of Technology

Tae Young Chung
Korea Institute of Machinery and Metals

Proceedings, ASME Winter Annual Meeting
Symposium on Flow-Induced Vibration
Chicago, December 1988

Abstract

Results are presented from a flow-induced vibration experiment conducted in a sheared current. The site was an historic 1848 mill canal with a width of 58 feet. Variable headgates allowed a controllable horizontal shear to be produced. An instrumented cable 1.125 inches in diameter was deployed horizontally in the flow. Response was measured for a variety of cable tensions and sheared flow profiles.

A method for predicting the response of cables in sheared flow is introduced, which includes the effects of correlation length, hydrodynamic damping, lift coefficient with higher order harmonics, and turbulence. Comparisons are made between predicted and measured response. The response is shown to contain significant amounts of vibration up to the fifth harmonic of the vortex shedding frequency. Hydrodynamic modal damping is shown to have a dramatic effect on the response, and to decrease with increasing frequency of vibration.

Nomenclature

$y(x,t)$	= cross flow response displacement
m	= structural mass per unit length including added mass
$R\frac{\partial y(x,t)}{\partial t}$	= damping force including hydrodynamic damping force
T	= tension
$f(x,t)$	= lift force per unit length due to vortex shedding
x	= response measurement point
ξ	= excitation point
T	= tension along the cable
k	= wave number$(=\omega/C_p)$
ω	= excitation frequency
ω_s	= local mean vortex shedding frequency at $x=\xi$
ω_s'	= local mean vortex shedding frequency at $x=\xi'$
b	= one standard deviation of the local mean vortex shedding frequency

C_p	= phase velocity of the cable($=\sqrt{\frac{T}{m}}$)
L_c	= the correlation length
L	= the cylinder length
l_c	$=L_c/L$ = coefficient determining the spatial correlation betweenξ and ξ'
$s.g.$	= specific gravity
ρ_w	= water density
D	= cylinder diameter
S_t	= Strouhal number
$V(x)$	= flow velocity at x
V_R	= reduced velocity
V_p	= peak velocity in a linear shear
ΔV_{rms}	= turbulence standard deviation
n	= mode number
N_s	= the number of modes excited by the linear sheared flow
ω_n	= natural frequency of mode n
ω_p	= natural frequency closest to the peak shedding frequency
Ψ_n	= mode shape
ς	= damping ratio
$\varsigma_{h,n}$	= hydrodynamic modal damping ratio
$\varsigma_{s,n}$	= structural damping ratio
ς_n	= total damping ratio
$R_{h,n}$	= hydrodynamic modal damping constant
B	= velocity squared damping coefficient
γ	= damping correction for response amplitude
H	= damping reduction factor
$C_L(x,t)$	= local, time varying lift coefficient
C_L^2	= mean square lift force coefficient
$C_{L,2}$	= coefficient of the 2nd harmonic
$C_{L,3}$	= coefficient of the 3rd harmonic
$S_{yy}(x,\omega)$	= the displacement response spectrum at location x
$S_{f_\xi f_{\xi'}}(\xi,\xi',\omega)$	= the lift force spectrum
$G(x/\xi)$	= the Green's function due to excitation at the location $x=\xi$
$G^*(x/\xi')$	= conjugate of the Green's function due to excitation at the location $x=\xi'$

1 Introduction

The prediction of the flow-induced vibration response of long, cylindrical structures deployed in sheared flows is a problem of considerable practical importance. The applications vary from extremely long cables that exhibit the dynamic behavior of systems of infinite length, Kim et al [5], to relatively short and stiff risers or pilings which respond to vortex shedding in only a few of the lowest natural modes of vibration. The authors have recently concluded a series of field tests using a 58-foot long, 1 1/8 inch diameter rubber hose, strengthened with longitudinal kevlar strands. The cable had a specific gravity with a flooded interior of 1.34. The cable was deployed in a controllable sheared flow. By varying the tension of the cable, dynamical properties of a wide variety of cylinders could be simulated. At high tensions, only a few of the lowest modes were excited, thus simulating the behavior of a short, nearly rigid riser. At very low tensions, the behavior of a rubber hose with many responding modes was observed. A response prediction model, based on the Green's function solution for the response of a cable to random excitation, was used in conjunction with a lift force cross spectrum model. The lift force cross spectrum model and the Green's function solution are both presented in detail in the paper. A description of the experiment is presented first, followed

by the response prediction model, and concluding with a comparison between measured and predicted response data, for a variety of combinations of shear profiles and cable tensions.

2 Shear Flow Experiments

2.1 Experiment Design

Experiments were conducted during the summer of 1986. A complete description, including many figures, may be found in References [2] and [12]. The test site was a mill canal, built in 1848 in Lawrence, Massachusetts. A dam diverts the water from the Merrimack River into the canal. The flow is controlled by four submerged gates, which are spaced at equal horizontal intervals beneath a gate house at the head of the canal. By controlling the various gate openings a sheared flow can be developed horizontally across the width of the canal, which is approximately 58 feet. The average depth of the canal is ten feet and the average flow rate for the experiments was from 200 to 750 cubic feet per second.

The test cable location was approximately 250 feet downstream of the gate house. The cable was tensioned horizontally across the width of the canal about one foot under the surface, as shown in Figure 1. Heavy steel pipe supports transferred the cable loads to the walls of the canal. Tension was applied to the cable via a system of pulleys and a hand- operated winch. For a given winch position the cable had essentially constant arc length. The tension then varied slowly with mean drag force on the cable. Tension was measured with a tension cell connected in series between the cable and winch.

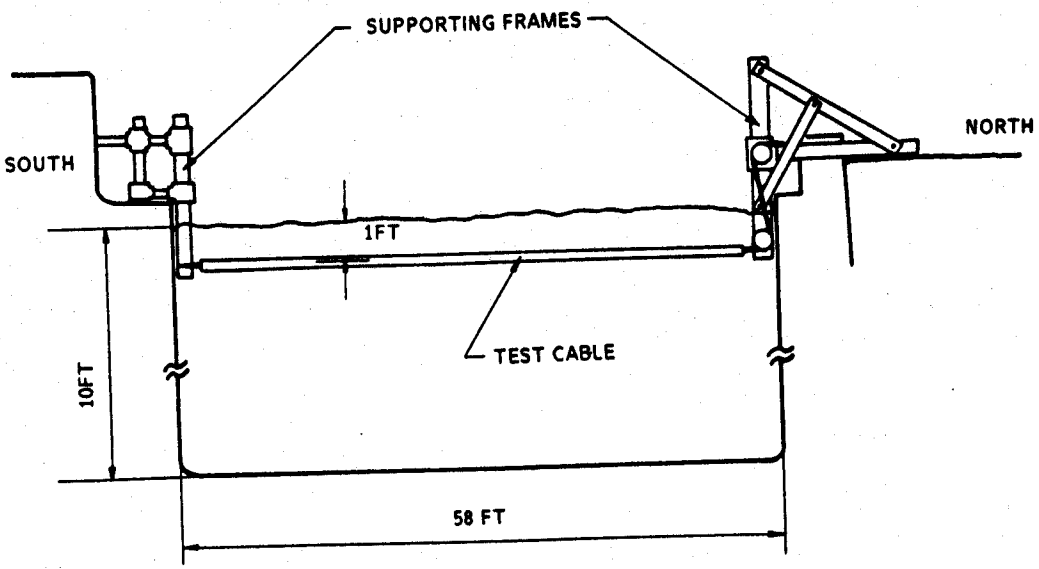

Figure 1 - Cable Deployment

Five feet upstream of the test cable, a simple traversing mechanism was constructed to carry a Neil Brown Instruments DRCM-2, two-axis acoustic current meter. The transducer was located about one foot under water and was oriented so that the instantaneous velocity was resolved into two components in the horizontal plane. The velocity was measured at two samples per second. The absolute accuracy of the device is better than 0.1 feet per second. The effective accuracy was less because drag forces prevented the current meter from hanging vertically. This would cause the measured values to be as much as 5 percent less than actual. The data shown have not been corrected for this error. It has no impact on the conclusions of this paper. The 58-foot long test cable is shown in Figure 2. It consisted of a 1.125 inch rubber hose with a 0.5 inch inside diameter. Seven 0.16 inch diameter braided kevlar cables were carried inside of the hose. Each kevlar cable had seven conductors inside of it. Three kevlar cables were used solely as load carrying members. Each one had an 800-pound breaking strength. Three cables were used to carry accelerometer signals and power, and one cable was used as a spare.

Six biaxial pairs of force balance accelerometers were placed on the centerline of the cable at locations shown in the figure. Each biaxial pair was 0.5 inches in diameter and 3 inches long. Space was created for the kevlar cables to pass around the accelerometers at these locations, with no change in the outside diameter of the hose. The accelerometers, tension cell, and current meter were the same as used in previous experiments conducted at Castine, Maine [10].

The 12 accelerometer outputs, tension, and current data were carried via a multi-conductor cable from the test cable to the gatehouse, where a Digital Equipment MINC-23 data acquisition computer was located. Fourteen data channels were digitized onto floppy disks at a data rate of 50 Hz per channel for low velocity tests and 60 Hz per channel for high velocity tests. A test run at 50 Hz acquired 4.8 minutes of data. A real time spectrum analyzer was used as an aid in determining the sampling rate necessary to guarantee no loss of important data and to prevent aliasing. Antialiasing filters were also used.

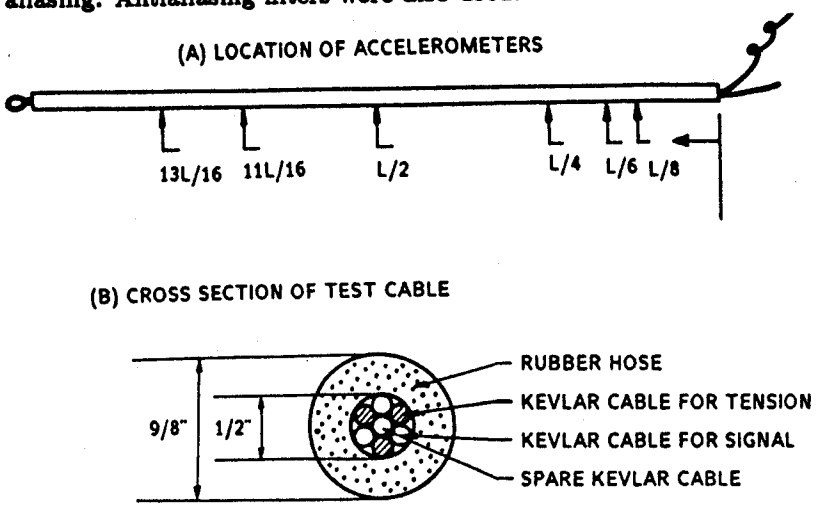

Figure 2 - Test Cable Construction

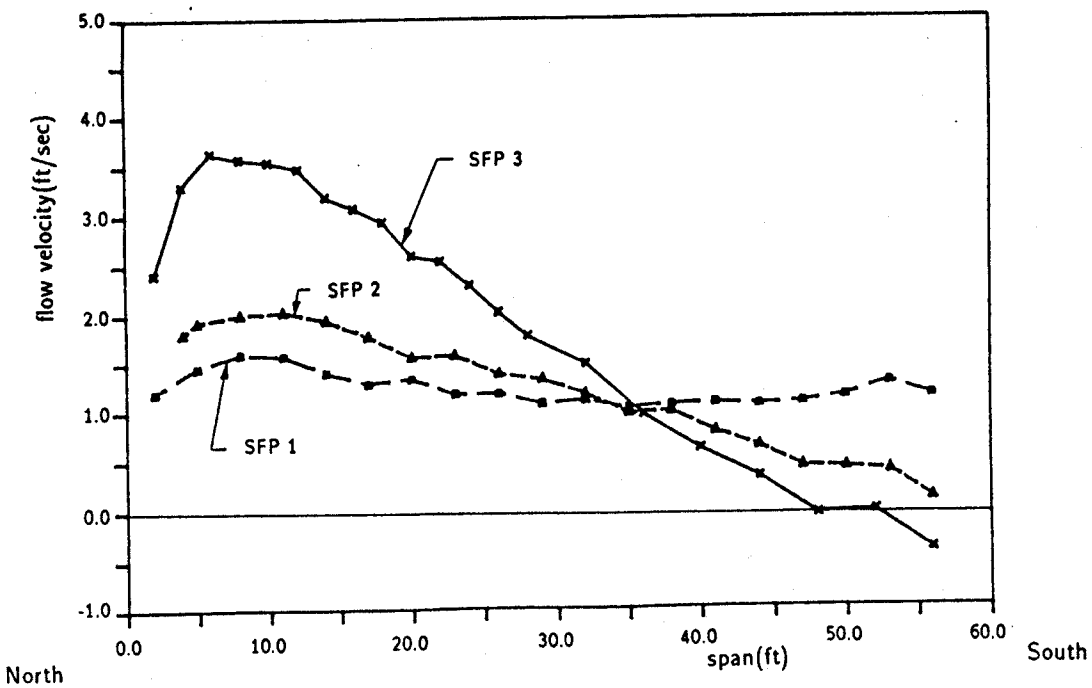

Figure 3 - Measured Current Profiles

2.2 Sheared Current Profiles

The current profiles were measured prior to response tests. The meter was traversed from one wall to the other in steps of 4 feet. At each location four minutes of data were taken. Mean and rms current values were determined for each location. During a vibration test, the current meter was stationed at one reference location, ten feet from the north wall. This was approximately the location of the maximum velocity in the shear profiles used.

The results of three different profiles are presented in this paper. They are shown in Figure 3. They are designated shear flow profile 1, 2, and 3 (SFP1, etc.). SFP3 was the steepest shear with a peak flow velocity at times exceeding 4 feet per second and a minimum flow velocity of -0.5 feet per second. The minus indicates reverse flow. SFP1 was made as close to uniform as possible by careful positioning of the gates. SFP2 ranged from 2 feet per second down to zero in a nearly linear profile. The flow was at all times highly turbulent. The rms turbulence level was from 10 to 20 percent of the maximum current in the profile. The time scale of the turbulence was up to several seconds in length. The lowest turbulence frequencies were associated with large eddies, up to 10 feet in diameter which were carried downstream from the gatehouse. Depending on the mean flow speed, these eddies took many seconds to pass the cable.

An important conclusion is that the turbulence did not alter greatly the vibration of the cable when compared in a subjective way to other experimental results, such as Castine, Maine [10]. The turbulence does make the vibration response have a broader frequency bandwidth, and was able to prevent pure, constant amplitude single mode lockin from occuring, even with the nearly uniform profile, SFP1.

3 A Response Prediction Model

3.1 Background

The vortex-induced vibrations of long-tensioned cylinders in uniform flow can be predicted reasonably well on the basis of experimental data. Examples are Sarpkaya 1979[8], Blevins 1977[1], and Griffin and Ramberg 1982[3]. A few attempts without experimental confirmation have been made to predict the response in a sheared flow. The prediction method used by Wang et al[14] was based on the superposition of a few lightly damped resonant modes, and the Patrikalakis and Chryssostomidis approach[6] uses hydrodynamic coefficients measured on oscillating cylinders in uniform flow. Neither approach was confirmed by experiments, and consequently are lacking in several important respects.

First, hydrodynamic modal damping is typically quite large under shear flow conditions[12]. As a consequence, mode superposition methods must include many non-resonant modes to correctly model spatial attenuation. Second, broad band vibration response dramatically reduces the coherence between cylinder motion and the dynamic properties of the wake directly behind it as shown in Shargel[9]. As a consequence, hydrodynamic coefficients measured on sinusoidally oscillating cylinders are inappropriate. Third, the lift force spectra must include significant energy at several higher order harmonics of the vortex shedding frequencies to adequately account for the high frequency cylinder response. Fourth, in mode superposition models, non-resonant modes are required to correctly obtain the spatial attenuation. Many modes may be required to obtain the correct solution. If the Green's function is available, it gives more accurate results with less computational effort because it is equivalent to a superposition of an infinity of modes.

The prediction of the response of a flexible cylinder to vortex shedding may be thought of as consisting of four major components: an excitation model, a structural model, a damping model, and a solution technique. All four components are addressed in the paper. A response prediction method is proposed for the vortex-induced vibration of long, tensioned cylinders in sheared flow, based on the Green's function approach.

3.2 A Proposed Linear Random Vibration Model of Exciting Force and Structural Response

The vortex shedding process excites the cable through a complex interaction, in which the motion affects the exciting forces in a poorly understood feedback mechanism. This is

especially important under single mode lockin conditions, for which the correlation between the vortex shedding process and the cylinder motion may be very high. However, under sheared flow, non-lockin conditions the correlation between cylinder motion and lift forces is very low and a simple non-feedback, random process model of the exciting forces can be successfully used to approximate the correct response. This is the approach used here.

Cylinder motions in the flow are a non-linearly correlated combination of cross-flow and in-line components. The correlation is due to a common source of excitation (the vortices) and not primarily due to mechanical coupling in the structure. The cross-flow response is typically much greater than the in-line response. The approach taken in this research is to compute the cross-flow response first, ignoring any influence of the in-line motion. If in-line motion is desired, then relationships discovered by Jong and Vandiver[13] may be used to predict it, after the cross-flow results are obtained.

Based on the preceding assumptions and arguments, a linear random vibration model is presented to predict the cross-flow vibration response of a tensioned cylinder to vortex shedding in a sheared flow.

In a linear one-dimensional continuous system, the displacement response spectrum at a location may be specified by the following integral equation:

$$S_{yy}(x,\omega) = \int_0^L d\xi \int_0^L d\xi' S_{f_\xi f_{\xi'}}(\xi,\xi',\omega) G(x/\xi) G^*(x/\xi') \tag{1}$$

where

$S_{yy}(x,\omega)$ = the displacement response spectrum at location x
$S_{f_\xi f_{\xi'}}(\xi,\xi',\omega)$ = the lift force spectrum
$G(x/\xi)$ = the Green's function due to excitation at the location $x = \xi$
$G^*(x/\xi')$ = conjugate of the Green's function due to excitation at the location $x = \xi'$

The mean square value of the response displacement at a location is obtained by integrating the displacement spectrum in the frequency domain.

$$E[y^2(x,t)]_{at\ x} = \int_0^\infty S_{yy}(x,\omega)\, d\omega \tag{2}$$

The Green's function of the system includes the structural modelling information as well as the hydrodynamic damping description. The lift force spectrum model includes all aspects of the hydrodynamic exciting forces. The solution technique used is a straightforward discrete numerical integration of equations (1) and (2).

3.3 Green's Function of a Finite Cable

The forced vibration of a finite cable with constant tension and uniformly distributed mass in a sheared flow can be described by an equation of motion.

$$m\frac{\partial^2 y(x,t)}{\partial t^2} + R\frac{\partial y(x,t)}{\partial t} - T\frac{\partial y^2(x,t)}{\partial x^2} = f(x,t) \tag{3}$$

where

$y(x,t)$ = cross-flow response displacement
m = structural mass per unit length including added mass
$R\frac{\partial y(x,t)}{\partial t}$ = damping force including hydrodynamic damping force
T = tension
$f(x,t)$ = lift force per unit length due to vortex-shedding

Fixed end boundary conditions are specified at x=0,L where L is the length of the cable.

In equation (3), $f(x,t)$ is varying in space and time. In order to get a solution for such conditions, the solutions to particular loadings in space and in time must be derived first. The response of the system at x to a unit harmonic force acting at a single point ξ is called the

Green's function. The extension to general loading in space is possible using the superposition principle.

The Green's function, $G(x/\xi)$, for the cable with damping is given by:

$$G(x/\xi) = \begin{cases} \frac{1}{T}\frac{\sin(k+ik\varsigma)x\sin(k+ik\varsigma)(L-\xi)}{(k+ik\varsigma)\sin(k+ik\varsigma)L} & (0 \le x < \xi) \\ \\ \frac{1}{T}\frac{\sin(k+ik\varsigma)\xi\sin(k+ik\varsigma)(L-x)}{(k+ik\varsigma)\sin(k+ik\varsigma)L} & (\xi < x \le L) \end{cases} \tag{4}$$

where

x = response measurement point
ξ = excitation point
T = tension along the cable
k = wave number$(= \omega/C_p)$
ω = excitation frequency
C_p = phase velocity of the cable$(= \sqrt{\frac{T}{m}})$

The response of the cable $y(x,t)$ to a unit harmonic force acting at ξ is thus:

$$y(x,t) = G(x/\xi)e^{-i\omega t} \tag{5}$$

The general forms of $\sin(x+iy)$ in equation (4) can be expressed in terms of their real and imaginary parts. Alternative forms of the Green's function and their derivations may be found in Chung, 1987[2].

When the exciting frequency is the same as the natural frequency of mode n, then it is interesting to investigate the resonant behavior of the Green's function for two extreme cases. One is the case when the resonant mode, n , and the damping ratio, ς , have small values so that the value of $n\varsigma$ satisfies the condition:

$$n\varsigma < 0.2 \quad \text{or} \quad n\pi\varsigma = \varsigma kL < 0.6 \tag{6}$$

Then, the first order approximation of the Green's function is given by:

$$G(x/\xi) = \frac{1}{T}\frac{\sin\frac{n\pi x}{L}\sin\frac{n\pi(L-\xi)}{L}}{\frac{n^2\pi^2}{L}\varsigma} \tag{7}$$

which is the same result one would obtain from normal mode superposition using only the response of the one resonant mode.

Another extreme is the case when the resonant mode number, n , has a larger value, the excitation point, ξ , and the response measurement point, x , are far from the end boundaries of the cable, and the damping ratio, ς, is less than 1. When these conditions are satisfied and the following condition is true

$$n\varsigma \gg 1 \quad \text{or} \quad n\pi\varsigma = \varsigma kL \gg \pi \tag{8}$$

then the Green's function is given by:

$$G(x/\xi) = \begin{cases} \frac{ie^{ik(\xi-x)}e^{-k\varsigma(\xi-x)}}{2Tk} & (0 \le x < \xi) \\ \\ \frac{ie^{ik(x-\xi)}e^{-k\varsigma(x-\xi)}}{2Tk} & (\xi < x \le L) \end{cases} \tag{9}$$

which is the same as the Green's function of an infinite cable, in which waves are damped out travelling from one end to the other.

Figure 4(A) shows an harmonic exciting force at the midpoint of a string at the natural frequency of the fifth mode. Figure 4(B) is a plot of the magnitude squared of the Green's function to that input when the modal damping ratio of the fifth mode is 1%. The Green's

function is an exact solution, equivalent to summing an infinite number of normal modes. However, in this case, a calculation of the response of the fifth mode contribution only would have appeared essentially the same. This response is typical of a "short" lightly damped cable. For this case $n\varsigma = 0.05(\varsigma kL = 0.05\pi)$.

Figure 4(C) is the response of the same string, excited by a unit force at the natural frequency of the 99th mode, with a modal damping of 10% ($n\varsigma = 9.9$ and $\varsigma kL = 9.9\pi$). This response is characteristic of an infinite cable response. Excitation at the mid-point is never felt at the ends. To get the right answer by mode superposition would have required well in excess of 100 modal contributions.

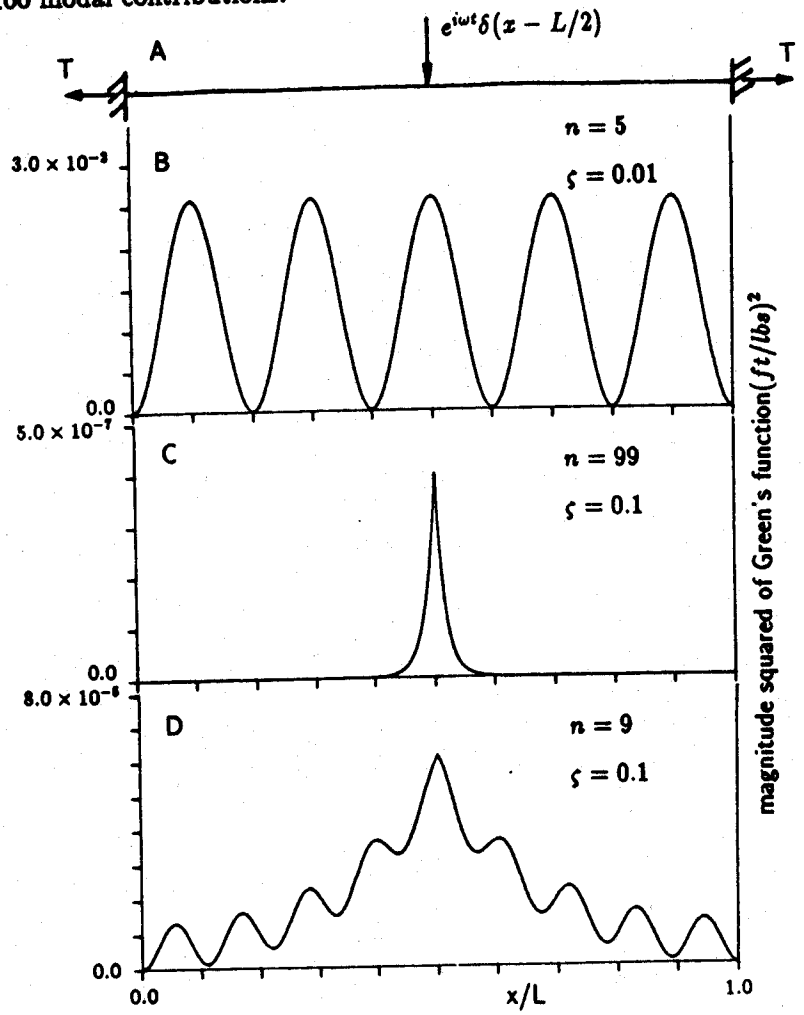

Figure 4 - The Green's Function for Three Cases of Damping and Mode Number

Figure 4(D) is for excitation at the ninth mode natural frequency with a damping of 10% ($n\varsigma = 0.9$ and $\varsigma kL = 0.9\pi$). Some vibration energy reaches the ends, but it is substantially damped.

The critical parameter to determine whether the cable acts like infinite cable or not is the product $n\varsigma$ where n is the mode number of the highest resonantly excited mode in the system. Three cases have been described here. In terms of this parameter they are

n	ς	$n\varsigma$	$n\pi\varsigma = \varsigma kL$
5	0.01	0.05	0.05π
9	0.10	0.9	0.9π
99	0.10	9.9	9.9π

When $n\varsigma$ is less than 0.2 then it is "short" in the dynamic sense used here and single mode resonant response will dominate the total response. Between 0.2 and 3 significant attenuation occurs over the length of the cable, but an infinite cable response model is not adequate. However, normal mode superposition may be used except that one may need from $2n$ to $3n$ terms because non-resonant modal contributions are essential in the correct solution. When $n\varsigma$ exceeds 3, then, except when excited near an end, the cable can be considered to behave dynamically as if it were infinite in length. When excited near an end, a semi-infinite model may be used. For $n\varsigma > 3$, mode superposition models are not very useful, because a large number of modes are required.

Another way of thinking of the quantity $n\varsigma$ is that $2n\varsigma$ is the number of modes contained within the half power bandwidth of mode n, for a constant tension uniform cylinder.

3.4 Hydrodynamic Damping Model

The practical, but approximate, hydrodynamic damping model used here is developed in detail in Reference[12]. A brief summary is presented here. At any specific location an instantaneous drag force per unit length may be defined as the force in the direction of the instantaneous relative fluid flow. The fluid velocity relative to the cable is the vector sum of the free stream velocity $V(x)$ and the negative of the local cross- flow cable velocity $\dot{y}(x,t)$. The in-line cable velocity $\dot{z}(x,t)$ is assumed small and is neglected (it could be included if a more precise estimate was required). If one assumes the drag force to be proportional to the relative velocity squared, then the magnitude of the drag force takes the form given below.

$$\mid F_D(x,t) \mid = \frac{1}{2}\rho_w C_D D(V^2 + \dot{y}^2) \tag{10}$$

Let,

$$B = \frac{1}{2}\rho_w C_D D$$

The component of the drag force in the y direction is by simple trigonometry given by

$$F_y(x,t) = -B\dot{y}\sqrt{V^2 + \dot{y}^2} \tag{11}$$

The damping force in equation (11) is a non-linear function of $\dot{y}$. It is helpful to find a linear equivalent damping constant $R(x)$ per unit length such that:

$$Damping\ \ force = -R(x)\dot{y} \tag{12}$$

An estimate can be obtained for a linear equivalent damping constant $R(x)$ for sinusoidal oscillations, if the requirement is imposed that the equivalent linear system dissipate the same energy per cycle as the non-linear one. In other words, it is required that

$$\frac{1}{T}\int_0^T R(x)\dot{y}^2 dt = \frac{1}{T}\int_0^T B\dot{y}^2\sqrt{V^2 + \dot{y}^2}dt \tag{13}$$

where T is one period of oscillation.

For values of $\dot{y}^2(x,t) \leq \frac{V^2(x)}{2}$ the linear equivalent damping takes the following approximate form.

$$R(x) = BV[1 + \frac{3}{8}\frac{\dot{y}^2}{V^2}] = \gamma BV(x) \tag{14}$$

where

$$\gamma \equiv [1 + \frac{3}{8}\frac{\dot{y}^2}{V^2}] \qquad 1.0 \leq \gamma \leq 1.2$$

R(x) is only weakly dependent on $\dot{y}$, and satisfactory results may be obtained by choosing an average value of $\dot{y}$ for the entire cable. This allows the parameter γ to be fixed for the entire cable. For all examples shown here, $\gamma = 1.0$. For cylinders which are excited in their low modes, the individual modal damping ratios are of interest. Equations (11) to (14) are still valid. However, the hydrodynamic modal damping constant, $R_{h,n}$, for mode n must be computed as follows

$$R_{h,n} = \int_0^L R(x)\Psi_n^2(x)dx \tag{15}$$

For constant tension uniform cables with pinned ends the mode shapes are given by

$$\Psi_n(x) = \sin(\frac{n\pi x}{L}) \tag{16}$$

Assuming a shear velocity which increases from zero linearly to a maximum value V_p

$$V(x) = V_p x/L \tag{17}$$

and

$$R(x) = \gamma B V_p x/L \tag{18}$$

where γ may be varied from 1.0 to 1.2 to account for the effect of $\dot{y}$ on $R(x)$, and V_p is the maximum or peak velocity in the flow. This discussion will proceed by first assuming that the damping acts over the entire cylinder. This will yield an upper bound on the modal damping constant. Substituting the expression for $R(x)$ in equation (18) into equation (15) and conducting the integral over the entire length yields for $R_{h,n}$ the following,

$$R_{h,n} = \gamma B V_p L/4 \tag{19}$$

The modal damping ratio is:

$$\varsigma_{h,n} = R_{h,n}/2\omega_n M_n \tag{20}$$

where M_n is the modal mass, $mL/2$, and ω_n is the predicted natural frequency in water including added mass effects. This reduces to

$$\varsigma_{h,n} = \frac{\gamma \rho_w C_D D V_p}{8\omega_n m} = \frac{\gamma C_D V_R(\omega_p/\omega_n)}{4\pi^2(s.g. + C_a)} \tag{21}$$

where the reduced velocity V_R is defined as $V_R = \frac{2\pi V_p}{\omega_p D}$. ω_p is the natural frequency which most closely corresponds to the peak flow velocity V_p with a reduced velocity of 5. Equation (21) may be used to estimate the hydrodynamic damping of any cable of finite length, constant tension, and constant diameter, in a linearly varying sheared flow of the type defined in equation (17). For the specific tests described in this paper, let

$$V_R = 5, \qquad C_a = 1.0 \qquad \text{and} \qquad s.g. = 1.34$$

then

$$\varsigma_{h,n} = 0.06\gamma C_D(\omega_p/\omega_n) \tag{22}$$

The damping is independent of mode number for the peak excited mode ($\omega_p = \omega_n$), and therefore $\varsigma_{h,p} = 0.06\gamma C_D$. Recall the parameter γ accounts for the increase in the damping constant due to the cylinders own motion and varies from 1 to about 1.2. Therefore, for a mean drag coefficient $C_D = 1.0$, the predicted maximum hydrodynamic damping ratio of the highest excited mode is from 6 to 8%. All lower modes are larger by the ratio ω_p/ω_n.

The expression in equation (19) for $R_{h,n}$ assumes that for any given mode, energy is lost to the fluid at all points on the cable. This contradicts the idea that there are regions of the cable where due to the coincidence of the vortex shedding frequency and a natural frequency substantial power flows into the cable and that less hydrodynamic modal damping should be included from such regions (Vandiver 1985[11], Wang et al 1986[14]). For the general sheared flow case, a more precise model of the hydrodynamic modal damping constant for mode n may be obtained by reducing the range of the integral in equation (15). If, from equation (15) we define the maximum modal damping as,

$$R_{h,n,max} = \int_0^L R(x)\Psi_n^2(x)dx \tag{23}$$

then $R_{h,n}$, as corrected, can be expressed as

$$R_{h,n} = H R_{h,n,max}$$

and

$$H = \frac{\int_0^{X_n - L_c} V(x)\Psi_n^2(x)dx + \int_{X_n+L_c}^{L} V(x)\Psi_n^2(x)dx}{\int_0^L V(x)\Psi_n^2(x)dx} \tag{24}$$

where $H \leq 1$ for all circumstances and X_n is the location most favorable for a resonant condition to exist between the vortex shedding process and mode n. L_c is the correlation length, or separation distance that causes the correlation between the lift forces at two locations to drop below a specified value. The correlation length is defined more precisely later in this paper. For now it is sufficient to say that a portion of cylinder $2L_c$ in length is the region into which most of the power will flow for mode n. Outside of this region will account for the dominant source of hydrodynamic damping for mode n.

For the linear sheared flow cases described in this paper, the correlation length coefficient, l_c , is defined by:

$$l_c = \frac{L_c}{L} \simeq \frac{1}{2N_s} \tag{25}$$

where

L_c = the correlation length
L = the cylinder length
N_s = the number of modes excited by the linear sheared flow

In other words, $2L_c$ is the distance on the cable which separates the locations at which the nth and n+1 natural frequency coincide with the mean vortex shedding frequency. For very long cables in a sheared flow for which N_s will be very large, then the ratio of the power-in region for each mode to total cylinder length, $2L_c/L$, will be very small and $H \simeq 1$.

For lower values of N_s the hydrodynamic modal damping ratio is obtained by estimating the value of H numerically:

$$\varsigma_{h,n} = H\varsigma_{h,n,max} = H\frac{R_{h,n,max}}{2\omega_n M_n} \tag{26}$$

The total damping ratio for the nth mode is the sum of hydrodynamic modal damping and structural damping for the nth mode:

$$\varsigma_n = \varsigma_{s,n} + \varsigma_{h,n} \tag{27}$$

3.5 Lift Force Spectrum Model

The excitation force per unit length in a sheared flow can be modelled as a spatially distributed random excitation (Kennedy 1979[4]):

$$f(x,t) = \frac{1}{2}\rho_w D V^2(x) C_L(x,t) \tag{28}$$

where

ρ_w = water density
D = cylinder diameter
$V(x)$ = flow velocity at x
$C_L(x,t)$ = local, time varying lift coefficient

If we assume that the local lift coefficient $C_L(x,t)$ is a random variable having the characteristics of being zero mean, Gaussian and time stationary-ergodic, then we can completely characterize the local lift coefficient by the space-time correlation function or its power spectrum. The lift force coefficient spectral model in a sheared flow should have a bandlimited spectrum centered on the dominant local vortex shedding frequency. This local spectrum should be correlated to that at neighboring locations by a spatial correlation function.

3.6 The Frequency Dependent Part of the Lift Coefficient

At any particular location, the peak frequency of the lift force coefficient spectrum corresponds to the local shedding frequency, $\omega_s(x)$:

$$\omega_s(x) = 2\pi S_t V(x)/D \tag{29}$$

Adopting a Gaussian description for the frequency dependent portion of the local lift force coefficient spectrum, the functional form appears as:

$$e^{-(\omega-\omega_s)^2/4b^2} \tag{30}$$

where

ω = excitation frequency (rad/sec)
ω_s = local mean vortex shedding frequency (rad/sec)
b = one standard deviation of the local mean vortex shedding frequency

However, experience has shown that higher harmonics appear in the response in both deterministic (lockin) and random response conditions. To account for this the model used here includes higher harmonic terms. Therefore the final form of the proposed local lift force coefficient spectrum is proportional to:

$$C_L^2(e^{-(\omega-\omega_s)^2/4b^2} + C_{L,2}e^{-(\omega-2\omega_s)^2/4(2b)^2} + C_{L,3}e^{-(\omega-3\omega_s)^2/4(3b)^2} + \cdots) \tag{31}$$

where

$C_{L,2}$ = coefficient of the 2nd harmonic
$C_{L,3}$ = coefficient of the 3rd harmonic
C_L^2 = mean square lift coefficient

The bandwidths of higher harmonics are assumed to increase in proportion to the center frequency.

3.7 Correlation Length Model

Ramberg and Griffin measured wake velocity signals behind vibrating flexible cables [7] and showed that under single mode lockin conditions the spatial cross-correlation coefficient between any two locations in the wake approached unity, being limited only by turbulence. However, in a sheared flow several modes can be excited simultaneously by the flow and the correlation length should be short and confined to regions in which the vortex shedding frequency closely corresponds to a resonant natural frequency of the cable. For the purposes of this paper the spatial cross- correlation of the lift force spectrum is probabilistically defined as a Gaussian random process with the correlation length corresponding to the standard deviation.

An alternative mathematical definition of the correlation length is given by Blevins [1] as a simple decaying exponential function. That form could also be used in place of the Gaussian one used here.

3.8 Lift Coefficient Spectrum

Combining these bandwidth and correlation length models leads to the following form of the lift coefficient spectrum.

$$\begin{aligned} S_{C_L}(\xi,\xi',\omega) \;=\; & \frac{C_L^2}{b\sqrt{2\pi}}\{e^{-(\omega-\omega_s)^2/4b^2} + C_{L,2}e^{-(\omega-2\omega_s)^2/4(2b)^2} + C_{L,3}e^{-(\omega-3\omega_s)^2/4(3b)^2} + \cdots\} \\ & \times\{e^{-(\omega-\omega_s')^2/4b^2} + C_{L,2}e^{-(\omega-2\omega_s')^2/4(2b)^2} + C_{L,3}e^{-(\omega-3\omega_s')^2/4(3b)^2} + \cdots\} \\ & \times e^{-(\xi-\xi')^2/2(l_cL)^2} \times sgn[G(x/\xi)G^*(x/\xi')] \end{aligned} \tag{32}$$

where

C_L^2 = mean square lift force coefficient
ω_s = local mean vortex shedding frequency at $x = \xi$
ω_s' = local mean vortex shedding frequency at $x = \xi'$
b = one standard deviation of the local mean vortex shedding frequency
$C_{L,2}$ = coefficient of the 2nd harmonic
$C_{L,3}$ = coefficient of the 3rd harmonic
l_c $= L_c/L$ = coefficient determining the spatial correlation between ξ and ξ'

The bandwidth of the excitation spectrum may depend on the turbulence of incident flow or it may depend on the motion of the cylinder and unsteady fluctuations in the vortex formation process. In a very low turbulence flow the lift force bandwidth on a stationary cylinder is very narrow. If the turbulence level is high (as it was at Lawrence) then we may expect the excitation bandwidth to depend on it, as estimated below. If one standard deviation of the local mean flow velocity due to turbulence is ΔV_{rms}, then the standard deviation of the local mean vortex shedding frequency in the lift force spectrum, b is given by:

$$b = 2\pi S_t \Delta V_{rms}/D = \Delta\omega_{rms} \tag{33}$$

For the Lawrence experiments the turbulence was 10 to 20% of the maximum current in the profile, and therefore dominated the bandwidth estimate.

Given the lift coefficient spectrum as defined in equation (32) the lift force spectrum can be written as:

$$S_{f_\xi f_{\xi'}}(\xi, \xi', \omega) = [\frac{1}{2}\rho_w V^2(\xi) D][\frac{1}{2}\rho_w V^2(\xi') D] S_{C_L}(\xi, \xi', \omega) \tag{34}$$

where

$S_{f_\xi f_{\xi'}}(\xi, \xi', \omega)$ = lift force spectrum
$V(\xi)$ = flow velocity at $x = \xi$
$V(\xi')$ = flow velocity at $x = \xi'$
ρ_w = water density
D = cylinder diameter
$S_{C_L}(\xi, \xi', \omega)$ = lift force coefficient spectrum

This model is used to predict the response observed in the Lawrence experiments.

4 Comparison of Predicted and Measured Response

The dynamic response characteristics of the test cable in sheared flows showed strong dependence on the velocity profile and the tension of the test cable. The tensions used in the prediction of response was the mean tension measured by the tension cell for a fixed position of the winch. Three different velocity profiles were emphasized in this research. They are shown in Figure 3 and are designated sheared flow profile 1, 2, and 3 (SFP1, etc.). For each sheared flow case, response with high and low tension was evaluated. The description for each test condition is summarized in Table 1. In the table each test condition is revealed by a number letter combination. For example, Test (1-H) represents the test carried out under the SFP1 profile and high tension, and Test (2-L) represents the test carried out under the SFP2 profile and low tension.

A few examples from this data set have been selected for this paper. The details of several others may be found in Reference [2].

4.1 Important Non-dimensional Parameters

The Reynolds numbers for all test conditions were in the subcritical region so that differences in Reynolds numbers between tests did not make significant differences in the dynamic response characteristics of the test cable. Reynolds numbers for each test are given in Table 2.

Table 1: Summary of the Experimental Test Conditions

Test condition	Test (1-H)	Test (1-L)	Test (2-H)	Test (2-L)	Test (3-H)	Test (3-L)
Sheared flow profile	Almost Uniform SFP1	Almost Uniform SFP1	Slightly Sheared SFP2	Slightly Sheared SFP2	Highly Sheared SFP3	Highly Sheared SFP3
Flow velocity (ft/sec)						
min.	1.0	1.0	0	0	-0.5	-0.5
max.	1.6	1.6	2.0	2.0	3.6	3.6
Vortex shedding frequency (Hz)*						
min.	1.8	1.8	0	0	0	0
max.	2.9	2.9	3.6	3.6	6.5	6.5
Tension (Lbs)	318	96	349	62	344	145
1st natural frequency (Hz)						
in air	1.16	0.64	1.22	0.51	1.21	0.78
in water**	0.88	0.48	0.92	0.38	0.91	0.59

*Vortex shedding frequencies were calculated from equation $f_s = S_t V/D$, where $S_t = 0.17$.
**An added mass coefficient of 1.0 was used in the calculation of the fundamental natural frequency in water.

Table 2: Dimensionless Parameters

Test condition	Test (1-H)	Test (1-L)	Test (2-H)	Test (2-L)	Test (3-H)	Test (3-L)
Flow profile	SFP1	SFP1	SFP2	SFP2	SFP3	SFP3
Tension (lbs)	318	96	349	62	344	145
Max. R_e (10^4)	1.4	1.4	1.7	1.7	3.1	3.1
Max. mode number $f_{s,max}/f_1$	3.3	6.0	3.9	9.5	7.1	11.0
Min. mode number $f_{s,min}/f_1$	2.0	3.8	1	1	1	1

The specific gravity of the test cable was 1.34. The test cable is a relatively low density structure. The lockin range expressed in reduced velocity terms is much broader for low density cylinders than for high density ones as discussed in Vandiver [11]. The cross-flow lockin of this test cable in a uniform flow would be expected to occur in the range of $3.5 \leq \frac{V}{f_n D} \leq 9$.

The most significant dimensionless parameter variations in these tests were in the maximum responding mode number, the number of modes participating in the response, and the damping. The cable tension determined the variation in modal separation or inversely the modal density. For a given modal density the amount of shear in the flow speed determined the number of excited modes and the frequency of the highest responding mode. The number of excited modes and the highest excited mode number are far more useful and provide more physical insight to the importance of the shear profile, than does the often used shear parameter. The damping had very large variation due to hydrodynamic effects.

For the six cases described here the values of nondimensional parameters for the test conditions are summarized in Table 2. The effective damping in water was estimated by two separate means, one experimental and one analytical. These are described in some detail in Reference [12]. The experimental determination was obtained by striking the cable impulsively with a pole and measuring the decay of the resulting pulse as it passed successive accelerometers. In that test the cable was also vibrating in response to the approximate uniform profile. The analytical estimation of hydrodynamic damping was obtained by assuming a drag coefficient and then calculating the damping force on the cable as presented in Section 3.4.

In air transient decay tests of the first few modes of the cable were conducted. For the tension ranges later used in water the structural damping was about 0.3%, which is negligible compared to the hydrodynamic losses experienced by the cable in sheared flow.

4.2 Implementation of the Response Prediction Model

A computer program was written to implement the response prediction method described earlier. Damping estimates were based on the hydrodynamic damping model presented earlier. The lift force spectrum was calculated at numerous discrete points in space and frequency. Using the estimated damping values and the lift force spectrum model, the displacement response spectrum at location x was obtained numerically:

$$\begin{aligned} S_{yy}(x,\omega_k) &= \int_0^L d\xi \int_0^L d\xi' S_{f_\xi f_{\xi'}}(\xi,\xi',\omega) G(x/\xi) G^*(x/\xi') \\ &= (\frac{L}{n_s})^2 \sum_{i=1}^{n_s}\sum_{j=1}^{n_s} S_{f_\xi f_{\xi'}}(i,j,\omega_k) G(x/i) G^*(x/j) \end{aligned} \tag{35}$$

where

$S_{yy}(x,\omega_k)$	=	the displacement response spectrum at location x and $\omega = \omega_k$
$\Delta\omega$	=	resolution in frequency domain
n_s	=	number of segments in the span L
L/n_s	=	resolution in space
$S_{f_\xi f_{\xi'}}(i,j,\omega_k)$	=	lift force spectrum at $\xi = \frac{iL}{n_s}$, $\xi' = \frac{iL}{n_s}$ and $\omega = \omega_k$
$G(x/\xi)$	=	the Green's function at x excited at $\xi = \frac{iL}{n_s}$
$G^*(x/\xi')$	=	conjugate of the Green's function at x excited at $\xi' = \frac{iL}{n_s}$

The acceleration spectrum is calculated from the displacement spectrum as shown below.

$$S_{\ddot{y}\ddot{y}}(x,\omega_k) = \omega_k^4 S_{yy}(x,\omega_k) \tag{36}$$

In order to confirm the validity of the present response prediction model for the non-lockin case, sample runs were made for four different test conditions and were compared with the experimental results. The values of input parameters used to determine hydrodynamic damping and hydrodynamic lift force are summarized in Table 3. Linear sheared flow profiles which closely approximated the experimental profiles were used in the prediction. C_D, C_a, and C_L were chosen to give good agreement with Test(2-H) and then kept at those values for all other cases. Resolution in space was $0.02L$ and resolution in frequency was $0.2Hz$ in the numerical calculation for all test conditions. All of the important outputs including the predicted and measured rms displacement are summarized in Table 4.

The measured acceleration spectra were averaged 14 times with record lengths of 1024 data points. The sampling frequencies were 50 Hz for Test(2-H) and Test(2-L)and 60 Hz for Test(3-H) and Test(3-L).

A comparison between predicted and measured response for two extreme cases will be shown. One is the high tension and low shear case (Test(2-H)) and the other is the low tension and high shear case(Test(3-L)).

The results for Test (2-H)(the slightly sheared flow, SFP2, and high tension) are shown in Figures 5 to Figure 8. The predicted acceleration spectra at the two locations, $x = L/8$ (high flow velocity region) and $x = 13L/16$ (low flow region), in Figure 5 do not show much spatial attenuation of the response. As discussed in section 3.3, $n\zeta_n$ is an important parameter in determining the cable's behavior. When $n\zeta_n$ is less than 0.2, single mode resonant response may dominate the total response. For Test (2-H) $n\zeta_n = 0.18$, and is therefore on the borderline in behavior. In this case the response was not lockin. The predicted result shows quite good agreement with the experimental results as shown in Figure 6 to Figure 8. Figure 8 shows the rms displacement response as a cumulative integral of the spectrum from high to low frequency. This reverse integration was done intentionally so as not to have to pick a low frequency cut off as a point to begin the integration.

Table 3: Summary of the model input parameters

Test condition	Test (2-H)	Test (2-L)	Test (3-H)	Test (3-L)
Flow profile	SFP2	SFP2	SFP3	SFP3
Flow velocity(ft/sec)				
min.	0	0	0	0
max.	2.00	2.0	3.5	3.5
One standard deviation of turbulence(ft/sec)	0.25	0.25	0.4	0.4
Tension (lbs)	349	62	344	145
Structural damping ratio	0.003	0.003	0.003	0.003
Drag force coeff. C_D	1.0	1.0	1.0	1.0
γ^*	1.0	1.0	1.0	1.0
Added mass coeff. C_a	1.0	1.0	1.0	1.0
Correlation length coeff. l_c^{**}	0.125	0.06	0.07	0.05
Mean square lift coeff. C_L^2	.631	.631	.631	.631
Coeff. of higher harmonics				
$C_{L,2}$	0.1	0.04	0.04	0.04
$C_{L,3}$	0.15	0.06	0.06	0.06
$C_{L,4}$	0.0025	0.001	0.001	0.001
$C_{L,5}$	0.025	0.01	0.01	0.01

* γ is the parameter which accounts for the effect of the response amplitude on the hydrodynamic damping. $\gamma = 1$ neglects the response amplitude effect on the hydrodynamic damping. This gives a lower bound estimate of damping for any assumed C_D.
** $l_c = \frac{1}{2n_{mas}}$ for each case

Table 4: Summary of the Predicted and Measured Response

Test condition	Test (2-H)	Test (2-L)	Test (3-H)	Test (3-L)
Flow profile	SFP2	SFP2	SFP3	SFP3
Flow velocity(ft/sec)				
min.	0	0	0	0
max.	2.00	2.0	3.5	3.5
Tension (lbs)	349	62	344	145
Calculated first natural freq.(Hz)	0.92	0.39	0.91	0.59
Standard deviation of excitation spectrum(Hz)	1.07	1.07	1.71	1.71
Peak mode number excited by the flow, n	4	9	7	11
Estimated damping ratio for the peak mode, ς_n	0.046	0.056	0.058	0.064
$n\varsigma_n$	0.18	0.50	0.41	0.70
Rms displ. at $x = L/8(in)$				
predicted	0.59	0.55	0.62	0.52
*measured**	0.57	0.45	0.51	0.50
Rms displ. at $x = 13L/16(in)$				
predicted	0.54	0.38	0.37	0.34
*measured**	0.53	0.46	0.39	0.41

* Low frequency cut-off for integration of acceleration spectra to get rms dispacement was 1.0 Hz.

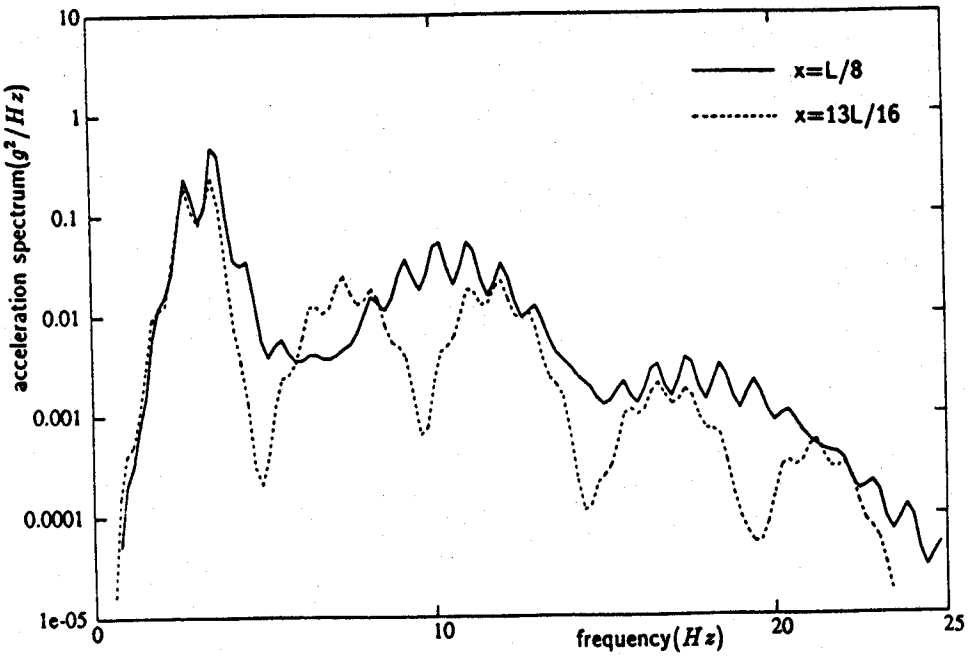

Figure 5 - Predicted Acceleration Spectra at L/8 and 13L/16 for Test(2-H)(slightly sheared flow, SFP2, and T=349 lbs)

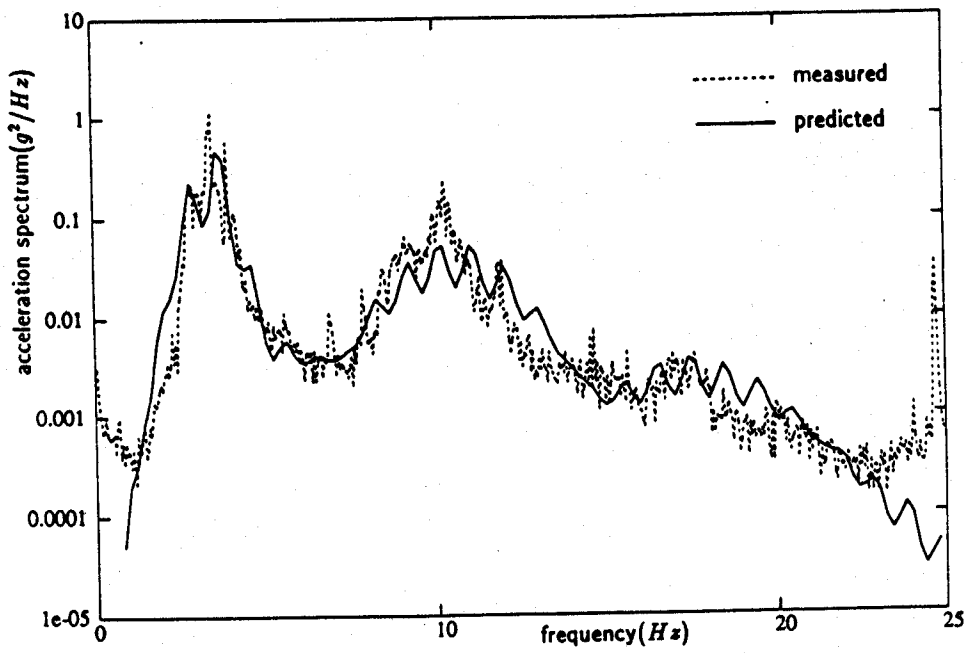

Figure 6 - Predicted and Measured Acceleration Spectra at L/8 for Test(2-H)(slightly sheared flow, SFP2, and T=349 lbs)

In Test (2-H) only 4 modes (1 through 4) were excited by the first harmonic of the lift force spectrum. The predicted damping for the first to the fourth modes was 24%, 13%, 6.8%, and 4.6%. for Test(2-H)(slightly sheared flow, SFP2, and T=349 *lbs*)

The results for Test (3-L)(the highly sheared flow, SFP3, and low tension)are shown in Figure 9 to Figure 12. The predicted acceleration spectra at the two locations, $x = L/8$ and $x = 13L/16$, as shown in Figure 9, reveal a large spatial attenuation of response. The estimated value of $n\varsigma_n$ was 0.7. For values of $n\varsigma_n$ between 0.2 and 3, significant spatial attenuation occurs

over the length of the cable. The predicted results for test (3-L) do not match as well as for test (2-H). The measured spectra are smoother and lack the predicted peaks and valleys. This is most likely due to large space and time variations in the flow velocity during the 4 minute data acquisition period. The prediction model assumed a stationary- ergodic excitation. The large actual variations in flow speed would tend to smear out the response spectrum measured at any one location. These non-stationary variations in flow conditions were worst in the highly sheared case.

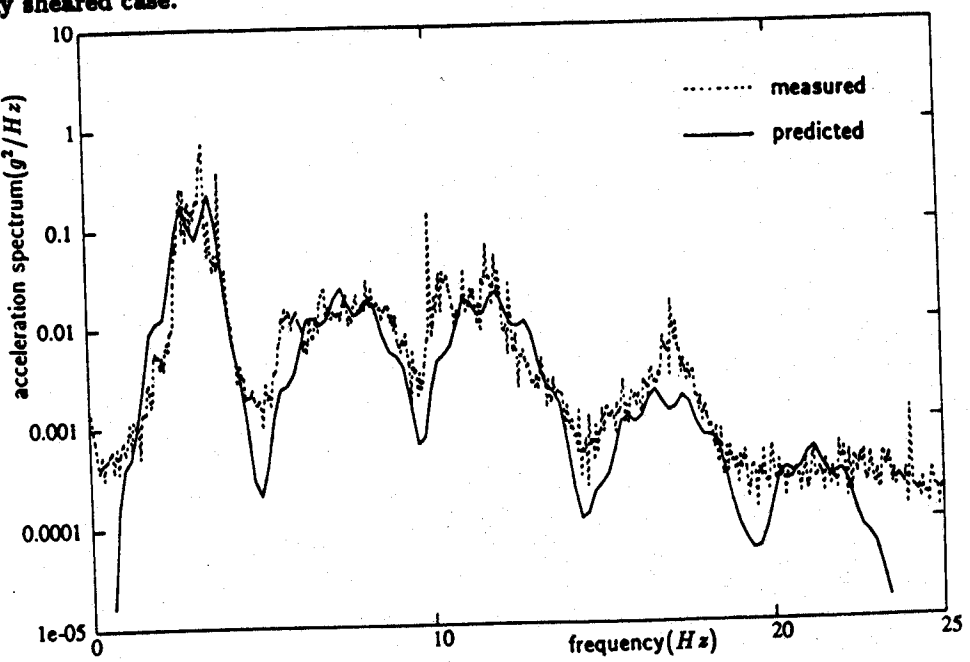

Figure 7 - Predicted and Measured Acceleration Spectra at 13L/16 for Test(2-H)(slightly sheared flow, SFP2, and T=349 lbs)

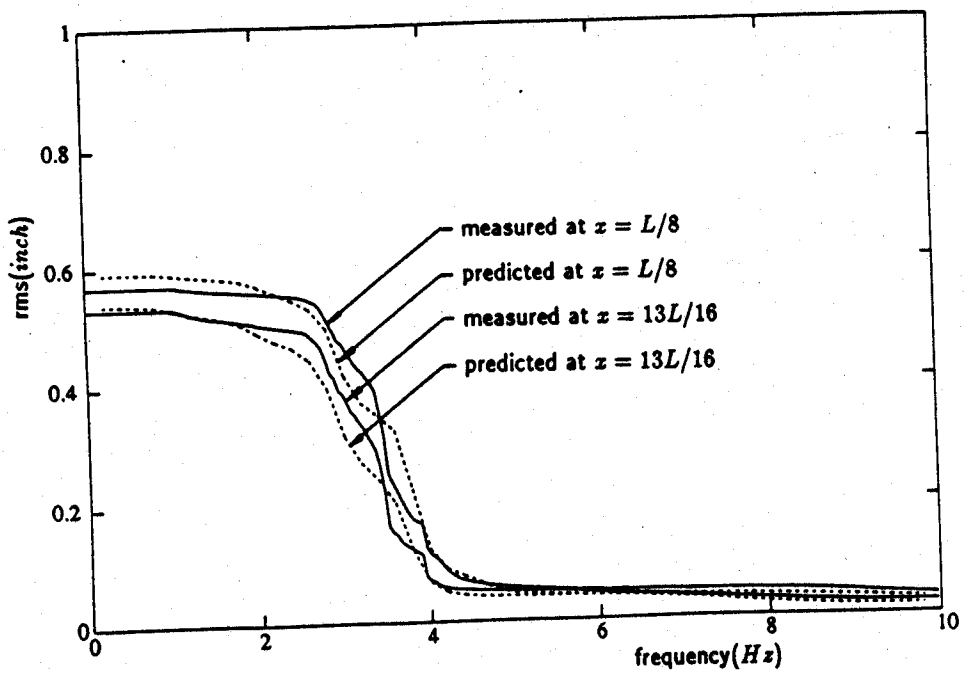

Figure 8 - Predicted and Measured Integrated Displacement Spectra at L/8 and 13L/16 for Test(2-H)(slightly sheared flow, SFP2, and T=349 lbs)

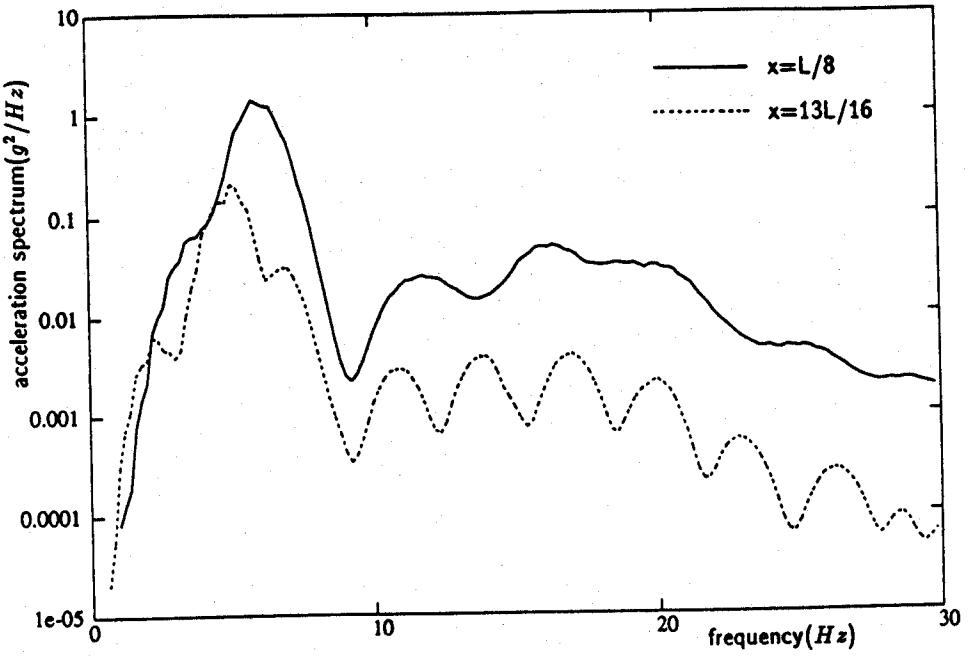

Figure 9 - Predicted Acceleration Spectra at L/8 and 13L/16 for Test(3-L) (highly sheared flow, SFP3, and T=145 lbs)

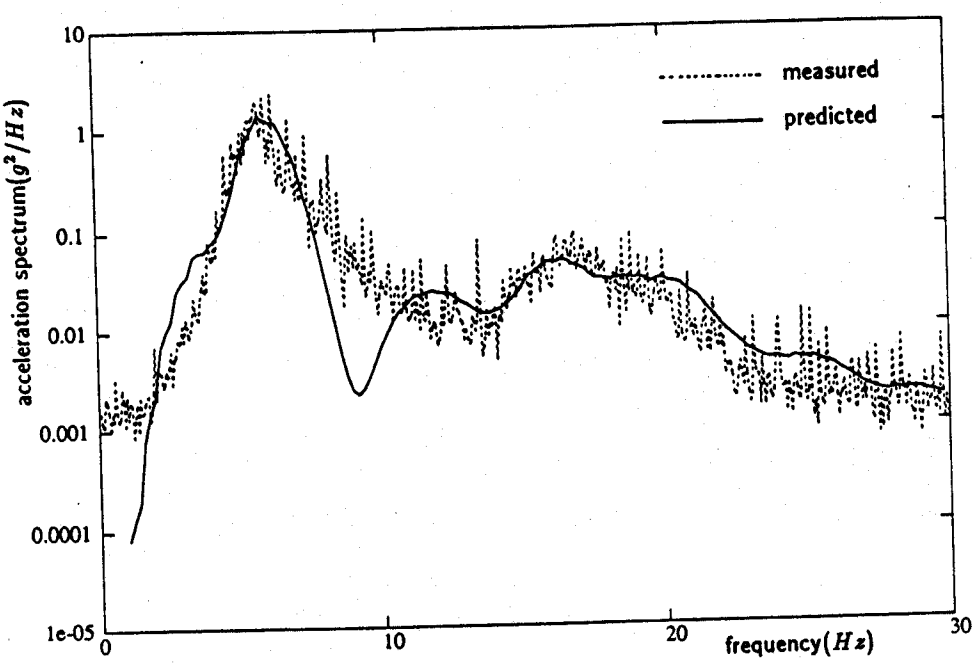

Figure 10 - Predicted and Measured Acceleration Spectra at L/8 for Test(3-L)(highly sheared flow, SFP3, and T=145 lbs)

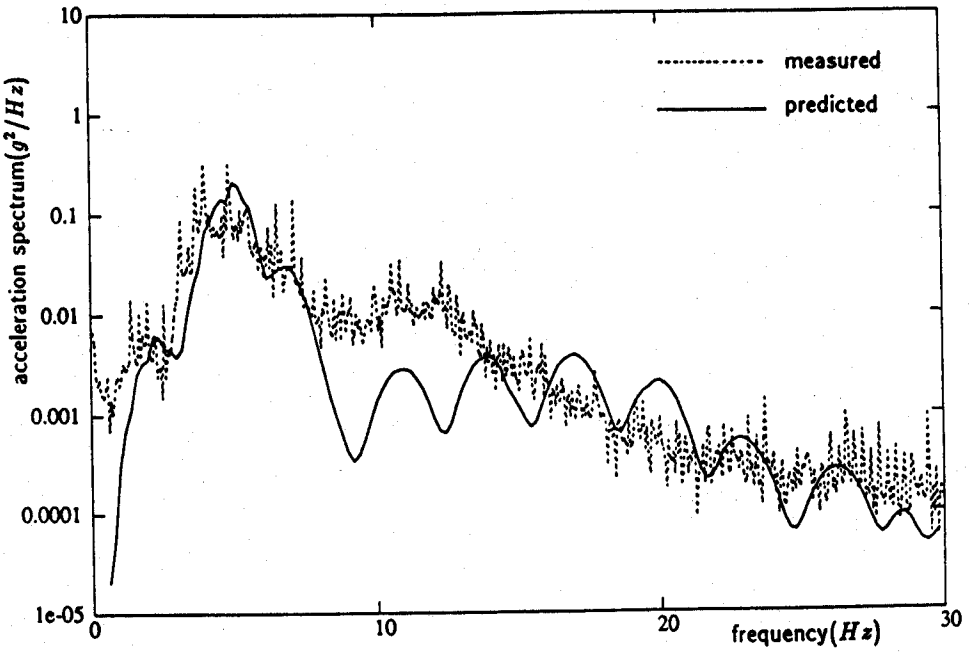

Figure 11 - Predicted and Measured Acceleration Spectra at 13L/16 for Test(3-L)(highly sheared flow, SFP3, and T=145 lbs)

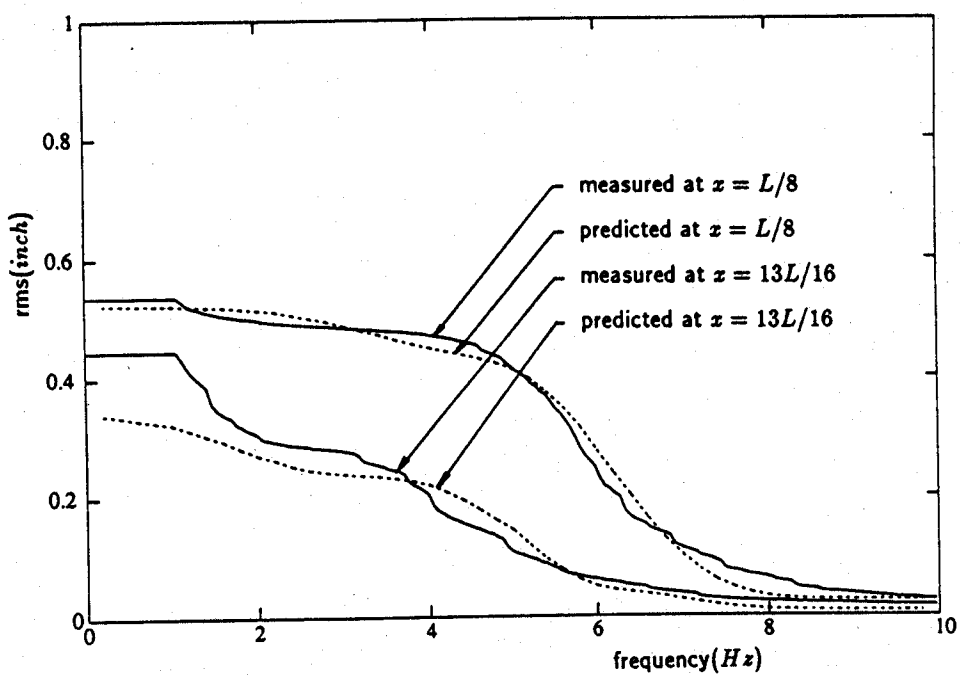

Figure 12 - Predicted and Measured Integrated Displacement spectra at L/8 and 13L/16 for Test(3-L)(highly sheared flow, SFP3, and T=145 lbs)

4.3 Parametric Study in C_L^2, C_D, ΔV_{rms}, l_c and ΔV_{rms}

A parametric study was undertaken to investigate the sensitivity of the predicted response due to variation in the mean square lift coefficient, C_L^2 , drag coefficient, C_D, variation in the standard deviation of turbulence, ΔV_{rms} , spatial correlation length coefficient, l_c , and variation in the maximum flow velocity of the sheared flow profile, V_{max}. Parametric studies were made for Test (3-L)(highly sheared flow, SFP3, and low tension) by varying one parameter and keeping the other parameters fixed. The values of input parameters used to carry out the sensitivity analysis, and the values of predicted rms displacement at x = L/8 are summarized in Table 5. More detail may be found in Reference [2].

Table 5: Prediction Model Sensitivity to Various Parameters

Input parameter	C_L^2	y^{**}_{rms}	C_D	y_{rms}	ΔV^{***}_{rms}	y_{rms}	l_c	y_{rms}	V^{****}_{max}	y_{rms}
1	0.158	0.19	0.5	0.67	0.2	0.46	0.025	0.41	3.0	0.53
2	.316	0.37	[1.0]	0.52	[0.4]	0.52	[0.05]	o.52	[3.5]	0.52
3	[.631]*	0.52	2.0	0.41	0.6	0.62	0.1	0.59	4.0	0.59

* The values in [ ] represent the values used in the prediction which came closest to the experimental observations.
** y_{rms} is in *inch* scale.
*** ΔV_{rms} is in ft/sec scale
**** V_{max} is in ft/sec scale

One additional sensitivity analysis emphasizing the higher order lift terms is best illustrated by Figure 13 which shows the predicted response with and without the higher order lift terms. Although small, the higher harmonics are important for acceleration prediction, such as for cables supporting acoustic transducers. The higher harmonics are not important in rms displacement response prediction.

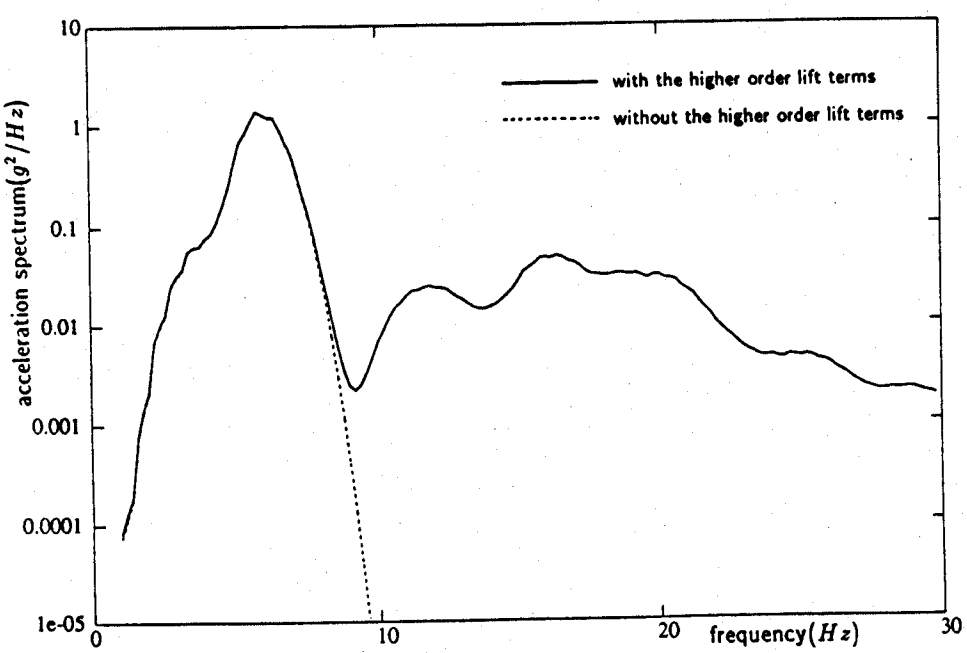

Figure 13 - Predicted Acceleration Spectra at L/8 for Test(3-L) With and Without the Higher Order Lift Terms

5 Summary and Conclusions

Field experiments were conducted to investigate the dynamic response characteristics of a tensioned cable in sheared flows. The tests were conducted under realistic field conditions with a length to diameter ratio of approximately 600. Uniform to highly sheared flows were achieved.

A response prediction method has been proposed for the non- lockin, vortex-induced vibration of a tensioned cylinder in sheared flow based on a Green's function approach. Hydrodynamic damping and lift force excitation models have been proposed based on linear random vibration theory. Response predictions have been compared to experimental observations.

Some of the more important findings are:

1. With the exception of pure, single mode lockin, hydrodynamic modal damping plays an important role in determining flow-induced vibration response. In these experiments hydrodynamic damping was 10 to 100 times larger than structural damping. For a given shear, the highest excited modes have the least damping.

2. The product $n\varsigma_n$, determines whether the cylinder behaves like a infinite cable or not. When this parameter exceeds 3, then infinite length behavior takes over. When it is less than 0.2, single modes may dominate the response. Though quantitative differences will exist, this conclusion is extendible to cylinders with bending stiffness and situations with spatially varying tension.

3. The mode superposition method requires many modes when $n\varsigma_n$ exceeds about 0.2. In such cases non-resonant modal contributions are substantial and account for the spatial attenuation.

4. The number of modes excited by the shear and the highest excited mode are more useful as dimensionless parameters than shear steepness, or the shear parameter.

5.1 Suggestions for Further Research

As an immediate extension of this work, it is suggested that the response prediction model be extended to cylindrical structures other than uniform cables with constant tension. Non uniform tension, diameter, and bending stiffness need all be considered. Correlation length models need further development and more research needs to be conducted to understand hydrodynamic damping mechanisms. The higher order lift coefficients used here were chosen to give good agreement between predicted and observed response. More research needs to be conducted to quantify their values.

6 Acknowledgements

This research was sponsored by Exxon Production Research, Shell Development Company, Chevron, Conoco, Unocal, the Naval Civil Engineering Laboratory, the Technology Assessment and Research Program of the Minerals Management Service, and the Naval Research Laboratory. Special thanks is given to the Lawrence Hydroelectric Associates for allowing us to use the canal and necessary facilities for conducting the experiments.

References

[1] R. D. Blevins. *Flow-Induced Vibration.* Van Nostrand Reinhold Co., 1977.

[2] T. Y. Chung. *Vortex-Induced Vibration of Flexible Cylinders in Sheared Flows.* Ph. D. Thesis, Massachusetts Institute of Technology, Ocean Engineering Department, May 1987.

[3] O. M. Griffin and S. E. Ramberg. "Some Recent Studies of Vortex shedding with Application to Marine Tubulars and Risers". *Journal of Energy Resources Technology,* Vol. 104, March 1982.

[4] M. B. Kennedy. *A Linear Random Vibration Model for Cable Strumming.* Ph. D. Thesis, Massachusetts Institute of Technology, Ocean Engineering Department, February 1979.

[5] Y. H. Kim, J. K. Vandiver, and R. A. Holler. "Vortex Induced Vibration and Drag Coefficients of Long Cables Subjected to Sheared Flows". *Journal of Energy Resources Technology*, Vol. 108, March 1986.

[6] N. M. Patrikalakis and C. Chryssostomidis. "Vortex-Induced Response of a Flexible Cylinder in a Sheared Current". *Journal of Energy Resources Technology*, Vol. 108, March 1986.

[7] S. E. Ramberg and O. M. Griffin. "Velocity Correlation and Vortex Spacing in the Wake of a Vibrating Cable". *Journal of Fluids Engineering*, Vol. 10, March 1976.

[8] T. Sarpkaya. "Vortex Induced Oscillations. A Selective Review". *ASME Journal of Applied Mechanics*, Vol. 46:pp 241–258, June 1979.

[9] R. S. Shargel. *The Drag Coefficients for a Randomly Oscillating Cylinder in a Uniform Flow.* M. S. Thesis, Massachusetts Institute of Technology, Department of Ocean Engineering, 1980.

[10] J. K. Vandiver. "Drag Coefficients of Long Flexible Cylinders". In *Proceedings of 1983 Offshore Technology Conference*, Houston, May 1983. OTC4490.

[11] J. K. Vandiver. "The Prediction of Lockin Vibration on Flexible Cylinders in a Sheared Flow". In *Proceedings of 1985 Offshore Technology Conference*, Houston, May 1985. OTC5006.

[12] J. K. Vandiver and T. Y. Chung. "Hydrodynamic Damping on Flexible Cylinders in Sheared Flow". In *Proceedings of 1987 Offshore Technology Conference*, Houston, May 1987. OTC5524.

[13] J. K. Vandiver and J. Y. Jong. "The Relationship Between In-Line and Cross- Flow, Vortex-Induced, Vibration of Cylinders". *Journal of Fluids and Structures*, Vol. 1, 1987.

[14] E. Wang, D. K. Whitney, and K. G. Nikkel. "Vortex-Shedding Response of Long Cylindrical Structures in Shear Flow". In *Proceedings Fifth International Symposium on Offshore Mechanics and Arctic Engineering*, Tokyo, April 1987.